Bioimpedance Simulations for the Monitoring of Fluid Overload in Heart Failure Patients

Alejandro Pliego Prenda[a], Alberto Olmo[b], Alberto Yúfera[c], Santiago F. Scagliusi[d], Pablo Pérez[e] and Gloria Huertas[f]

Instituto de Microelectrónica de Sevilla, Universidad de Sevilla, Dto. Tecnología Electrónica, ETSII, Seville, Spain

Keywords: Bioimpedance, Simulation, Cole Model, Dielectric Properties, in Vivo, Frequencies, Heart Failure.

Abstract: Heart Failure (HF) is a relevant disease that leads to an overload of fluids (edema) that accumulate in the pulmonary and systemic vascular territory of the patient. The use of bioimpedance measurements have been proposed for the monitoring of edema in heart failure patients, being necessary to optimize the design of electrodes systems in medical medices. In our work we present the modelling of the supramalleolar section of the leg, and finite element simulations of bioimpedance measurements performed to monitor fluid overload in lower limbs. Results show the similarity of our simulations with performed experiments, and the validity of our model to study the optimization in the design process of bioimpedance electrodes.

1 INTRODUCTION

Heart Failure (HF) is a major cause of illness, death, and use of health care resources. Currently, an estimated 64.3 million people are living with heart failure worldwide (Groenewegen et al., 2020). HF is characterized by symptoms and signs that result from abnormalities in cardiac structure and its function. In most cases, HF is preceded, not by an acute change in cardiac activity, but by retention of interstitial fluid which, accumulating in the pulmonary and systemic vascular territory, results in systemic congestion that eventually causes organ dysfunction due to hypoperfusion (decreased blood flow through an organ) (Arrigo et al., 2020). However, one of the earliest manifestations of heart failure is the accumulation of interstitial fluid in the feet and ankles, as these are regions farther away from the body center, which hinders venous return, and for this reason, increased ankle volume is commonly used as a noninvasive indicator of arterial stiffness which is closely related to heart failure (Gupta et al., 2014).

The standard assessment of HF (signs and symptoms, imaging tests and measurement of natriuretic peptides) generally does not reliably predict the appearance of a decompensation. Other methods for the edema assessment such as the water displacement method are quite reliable, however they are time-consuming and require the continuous presence of medical personnel to carry out the measurement (Brodovicz et al., 2009).

Recently, the electrical bioimpedance of biological materials has been widely used for the characterization of cells, tissues and organs, representing an excellent marker for obtaining information for medical diagnosis (Khalil et al., 2014), (Różdżyńska-Świątkowska et al., 2015).

The use of bioimpedance measurements have also been proposed for the monitoring of edema in heart failure patients. Some electronic devices such as SFB7 (impedimed, 2022) or MoinstureMeterD (Delfin Technologies, 2022) have been developed to be able to determine the water content present in biological tissues by means of bioimpedance measurements, which are non-invasive methods, but their use is limited to hospitals as they are non-portable devices. In addition, different wearable devices for the real time monitoring of acute heart fail patients have been developed and tested (Puertas et al., 2021). However, it is necessary to perform a thorough study of the system of electrodes used, in order to optimize the bioimpedance monitoring of edema evolution, and identify the possible use in the prognosis of the dis-

[a] https://orcid.org/0000-0001-8873-7063
[b] https://orcid.org/0000-0001-6388-4462
[c] https://orcid.org/0000-0002-1814-6089
[d] https://orcid.org/0000-0002-5634-5126
[e] https://orcid.org/0000-0001-7283-7254
[f] https://orcid.org/0000-0001-5851-2576

Prenda, A., Olmo, A., Yúfera, A., Scagliusi, S., Pérez, P. and Huertas, G.
Bioimpedance Simulations for the Monitoring of Fluid Overload in Heart Failure Patients.
DOI: 10.5220/0011744700003414
In *Proceedings of the 16th International Joint Conference on Biomedical Engineering Systems and Technologies (BIOSTEC 2023) - Volume 1: BIODEVICES*, pages 164-168
ISBN: 978-989-758-631-6; ISSN: 2184-4305

ease.

In our work, we study a specific configuration of electrodes for the monitoring of fluid overload with bioimpedance measurements. We model the supramalleolar section of the leg, and perform finite element simulations of the volume increase due to fluid accumulation in the extracellular space of muscle tissue (edema), in order to verify the applicability of the technique and the optimal range of frequencies. A bioimpedance 4 electrodes system is studied, in order to compare the simulations performed with the electrical measurements presented in (Puertas et al., 2021), and validate the utility of our model.

2 MATERIALS AND METHODS

The geometry of the model is based on an idealisation of the problem, assuming the supramalleolar segment of the leg as a succession of symmetrical, 15 cm high, cylinders with the same axis of symmetry. Each one of these cylinders corresponds to a different type of tissue and, therefore, their width must obey to a realistic physiological ratio.

For this reason, a radius of 10 mm has been taken to characterise the bone tissue, 25 mm thick for the muscle tissue, 5 mm thick for the adipose (fat) tissue and 1 mm thick to characterise the dermis (skin) layer. For these values, a study carried out in COMSOL on body thermostimulation was used as a reference (Kocbach et al., 2011). In addition, a distinction is made between two different regions of the bone due to their resistive characteristics: the cortical bone region, which is more external and 2 mm thick, and the cancellous bone, with a radius of 8 mm, which is contained inside the previous region (Du et al., 2018). Finally, four cylinder shaped electrodes with a radius of 5 mm and a height of 1 mm will stay over the skin, placed at the vertices of a rectangle with 6 cm high and 3.5 cm wide.

On the other hand, the electrodes material has been considered to be 304 stainless steel, because this is the most common type of steel, whose conductivity and relative permittivity are respectively $\sigma = 1.39 \cdot 10^6$ S/m and $\varepsilon_r = 1.008$ (MatWeb, 2022) practically constant for all frequencies.

The Cole-Cole equation shows, for a material, its complex relative permittivity ($\hat{\varepsilon}$) as the sum of several terms: the relative permittivity at high frequencies (ε_∞), the sum of complex relative permittivity for each dispersion region (frequency ranges over which conductivity and permittivity are practically linear) and the term associated with the static ionic conductivity (Gabriel et al., 1996).

$$\hat{\varepsilon}(\omega) = \varepsilon_\infty + \sum_{n=1}^{4} \frac{\Delta\varepsilon_n}{1 + (j\omega\tau_n)^{(1-\alpha_n)}} + \frac{\sigma_i}{j\omega\varepsilon_0} \quad (1)$$

Where $\Delta\varepsilon_n$, τ_n and α_n are respectively the range of permittivities, the time constant and the distribution parameter for each relaxation region. σ_i is the static ionic conductivity of the material and ε_0 is the vacuum permittivity. The above data can be found in Table 1.

$$\varepsilon_r(\omega) = \Re(\hat{\varepsilon}(\omega)) \quad (2)$$

$$\sigma(\omega) = \varepsilon_0\omega\Im(\hat{\varepsilon}(\omega)) \quad (3)$$

Complex relative permittivity $\hat{\varepsilon}(\omega)$ obtained by (1) contains a material information about its relative permittivity $\varepsilon_r(\omega)$ (real part) and its electrical conductivity $\sigma(\omega)$ (proportional to the imaginary part) for any frequency value.

The implementation of the physics requires the use of the electrical current package provided by COMSOL. Two of the electrodes were set with a normal current density J_n to the surface such that the current I supplied to the body was 0.1 and -0.1 mA, taking into account the radius of the electrode according to (3), where r is the radius.

Another electrode was connected to ground ($V = 0$) to measure on the remaining electrode. The electrical isolation of the whole system as well as the conservation of current must also be taken into account, since it is assumed that the system is electrically isolated from the external medium. This simulation has been studied for a set of frequencies with 17 measurements between 10 Hz and 1000 kHz.

$$J_n = \frac{I}{\pi r^2} \quad (4)$$

Finally, an extremely fine mesh is selected, i.e. where the tetrahedra on which the equations of the physical system will be solved will be very small, in order to obtain the results as accurately as possible.

In the study following to the creation of the COMSOL simulation, the surface integral of the current density at an electrode with initial current conditions is taken. With this data, the actual current and the surface integral of the voltage (divided by the area of the electrode), can be obtained to get the voltage V. Then, knowing the current and voltage, it is possible to obtain the bioimpedance measurement, and separate its data into the resistance R and the reactance X, values with which to plot the Cole diagram, showing the reactance versus resistance values of the system for a given frequency range.

$$\frac{V}{I} = Z = R + jX \quad (5)$$

Table 1: Data for each material for the relative permittivity at high frequencies ε_∞, the static ionic conductivity σ_i and, for each one of the scattering regions, the range of permittivities $\Delta\varepsilon_n$, the time constant τ_n and the distribution parameter α_n. Of all the tissue materials available in (Różdżyńska-Świątkowska et al., 2015), the following materials have been selected: for fat, non-infiltrated over infiltrated, and for skin, dry over wet.

	Cancellous bone	Cortical bone	Muscle	Fat	Skin (dry)
ε_∞	2.5	2.5	4.0	2.5	4.0
$\Delta\varepsilon_1$	18.0	10.0	50.0	3.0	32.0
$\tau_1\,(ps)$	13.26	13.26	7.23	7.96	7.23
α_1	0.22	0.20	0.10	0.20	0.00
$\Delta\varepsilon_2$	300	180	$7\cdot10^3$	15	1100
$\tau_2\,(ns)$	79.58	79.58	353.68	15.92	32.48
α_2	0.25	0.20	0.10	0.10	0.20
$\Delta\varepsilon_3$	$2.0\cdot10^4$	$5.0\cdot10^3$	$1.2\cdot10^6$	$3.3\cdot10^4$	0.0
$\tau_3\,(\mu s)$	159.15	159.15	318.31	159.15	
α_3	0.20	0.20	0.10	0.05	
$\Delta\varepsilon_4$	$2.0\cdot10^7$	$1.0\cdot10^5$	$2.5\cdot10^7$	$1.0\cdot10^7$	0.0
$\tau_4\,(ms)$	15.915	15.915	2.274	7.958	
α_4	0.00	0.00	0.00	0.01	
$\sigma_i\,(S/m)$	0.0700	0.0200	0.2000	0.0100	0.0002

3 RESULTS

In Figure 1, a representation of the equipotential lines for the electric field denoted in coloured lines is shown, with the direction and relative intensity of the electric current marked with red arrows.

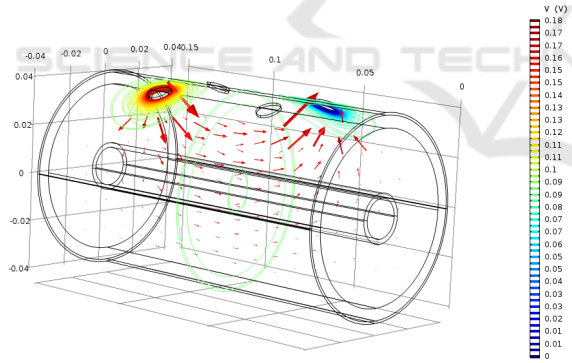

Figure 1: Equipotential lines for the electric field.

The result shown in Figure 1 is consistent with what would be expected. A current that is transmitted mainly through the most superficial layers of the ankle, but which penetrates down to the muscle, avoiding the cortical bone region, through which practically no current circulates since, given its low conductivity, it acts practically as an electrical insulator.

According with the stipulations of the procedure, the voltage and current data and their associated impedance for the different frequency values at which this current is supplied are shown in Table 2.

The different impedance values obtained for the different frequencies are shown in Figure 2. The Cole diagram (Figure 3) of the system is obtained by plotting the imaginary part (with opposite sign) against the real part of the impedance for different frequency values (Puertas et al., 2021).

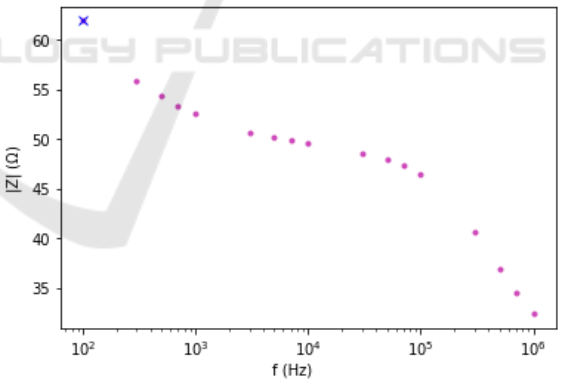

Figure 2: Impedance vs frequency sweep.

The Cole diagram (Figure 3) shows the typical semicircle characterising the material, but with a prolongation on the right part, corresponding to lower frequencies. This prolongation (corresponding to frequencies from 1 Hz to 5 kHz in our simulations) is not shown in empirical data (Puertas et al., 2021), where a lower frequency of 1 kHz was used. We can also see a general increase in the simulated values respect the experimental ones. Based on empirical data obtained from in vivo tests on healthy individuals, the semicircle should form in a range of resistances between

Table 2: Values of voltage (V), current (I) and impedance (Z) for different frequencies (f) obtained by simulation.

Frequency (Hz)	Voltage (mV)	Current (mA)	Impedance (Ω)
$1 \cdot 10^2$	$-6.10 + 1.12j$	-0.1002	$60.83 - 11.49j$
$3 \cdot 10^2$	$-5.57 + 0.64j$	-0.1002	$55.54 - 6.39j$
$5 \cdot 10^2$	$-5.43 + 0.52j$	-0.1002	$54.12 - 5.17j$
$7 \cdot 10^2$	$-5.33 + 0.45j$	-0.1002	$53.39 - 4.52j$
$1 \cdot 10^3$	$-5.25 + 0.39j$	-0.1002	$52.39 - 3.92j$
$3 \cdot 10^3$	$-5.07 + 0.24j$	-0.1002	$50.46 - 2.43j$
$5 \cdot 10^3$	$-5.02 + 0.21j$	-0.1002	$50.07 - 2.17j$
$7 \cdot 10^3$	$-4.99 + 0.21j$	-0.1002	$49.78 - 2.06j$
$1 \cdot 10^4$	$-4.96 + 0.21j$	-0.1002	$49.49 - 2.06j$
$3 \cdot 10^4$	$-4.86 + 0.28j$	-0.1002	$48.47 - 2.84j$
$5 \cdot 10^4$	$-4.79 + 0.37j$	-0.1002	$47.76 - 3.73j$
$7 \cdot 10^4$	$-4.72 + 0.45j$	-0.1002	$47.08 - 4.55j$
$1 \cdot 10^5$	$-4.62 + 0.56j$	-0.1002	$46.05 - 5.60j$
$3 \cdot 10^5$	$-4.00 + 0.83j$	-0.1002	$39.80 - 8.34j$
$5 \cdot 10^5$	$-3.62 + 0.79j$	-0.1002	$36.04 - 7.95j$
$7 \cdot 10^5$	$-3.40 + 0.71j$	-0.1002	$33.84 - 7.08j$
$1 \cdot 10^6$	$-3.21 + 0.57j$	-0.1002	$31.90 - 5.74j$

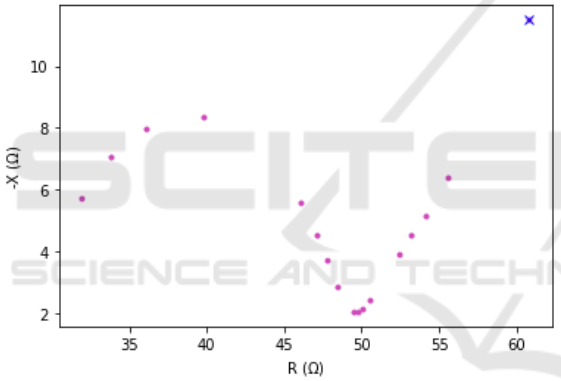

Figure 3: Cole diagram.

35 and 60 Ω (Puertas et al., 2021). This range is relatively close to the one obtained in our simulations, validating the use of the implemented model for these studies.

4 CONCLUSIONS

In our work we propose the use of finite element simulations for the study of the monitoring of fluid overload with bioimpedance measurements in heart failure patients. We have modelled the supramalleolar section of the leg, and performed finite element simulations for the bioimpedance measurements of the 4 electrode system used in (Puertas et al., 2021).

Results show a similar behaviour with the Cole-Cole model, being only different at lower frequencies. The differences with respect to performed experiments may derive from an excess of idealization when constructing the model, where perfect contact between the skin and the electrodes is assumed and spatial differences due to the asymmetry of the real leg are not taken into account. On the one hand, it would be necessary to continue working on improvements to the model to make it more realistic, but on the other hand, we believe it is necessary to have more clinical trials that could provide useful measuring for experimental development.

The supramalleolar section of the leg model presented can be an interesting model to simulate different types of electrode systems, and optimize the design of wearable electrodes for the monitoring of fluid overload in heart failure patients. The use of the ankle for measuring is advantageous compared to measurements taken on the whole body or on other body segments, since the onset of peripheral edema (as a precursor of HF) is earlier in the lower extremities of the body and the ankle is also a comfortable and discreet area to carry a measuring device all day long, thus allowing for continuous monitoring of the patient.

Simulation works like ours can be really useful, not only for this device, but also to improve the design of other bioimpedance measuring instruments, allowing to study the most optimal shape and arrangement of the electrodes before designing the prototype, which will give better results.

5 FUTURE STEPS

The presented model proves that it is possible to model bioimpedance measurements using the finite element method and lays the groundwork for future biomedical device modeling. Our long-term goals are, firstly, to continue with the cylindrical model, as it is a simple way to correlate the increase in volume due to swelling by fluid accumulation with the effect on the measured bioimpedance, but on the other hand, we also aim to move towards more realistic models, where we are considering using cross-sectional images of the ankle section or even three-dimensional tomographies of the leg, so that we can carry out studies thanks to which we can even indicate the best way of placing the measuring device, taking into account the proximity of the bones, the fat accumulation in a certain area or other factors. However, our most immediate objective is to validate the data obtained from the simulation with experimental results, so that we can be sure that the model adjusts to the behavior of the device on healthy individuals and, subsequently, on diseased patients.

ACKNOWLEDGEMENTS

This work was supported by the Spanish-funded project: “PRototipado y Ensayo CLÍnico del nuevo dispositivo portátil HFvolum para la monitorización en tiempo real de volúmenes en pacientes con insuficiencia cardiaca (PRECLI-HF)”, AT 21_00010, funded by Junta de Andalucía – Consejería de Transformación Económica, Industria, Conocimiento y Universidades.

REFERENCES

Arrigo, M., Jessup, M., Mullens, W., Reza, N., Shah, A. M., Sliwa, K., and Mebazaa, A. (2020). Acute heart failure. *Nature Reviews Disease Primers*, 6(1):1–15.

Brodovicz, K. G., McNaughton, K., Uemura, N., Meininger, G., Girman, C. J., and Yale, S. H. (2009). Reliability and feasibility of methods to quantitatively assess peripheral edema. *Clinical medicine & research*, 7(1-2):21–31.

Delfin Technologies (2022). https://delfintech.com/ moisturemeterd.

Du, W., Zhang, J., and Hu, J. (2018). A method to determine cortical bone thickness of human femur and tibia using clinical ct scans. In *2018 IRCOBI conference proceedings, Athens (Greece)*, pages 403–412.

Gabriel, S., Lau, R., and Gabriel, C. (1996). The dielectric properties of biological tissues: Iii. parametric models for the dielectric spectrum of tissues. *Physics in medicine & biology*, 41(11):2271.

Groenewegen, A., Rutten, F. H., Mosterd, A., and Hoes, A. W. (2020). Epidemiology of heart failure. *European journal of heart failure*, 22(8):1342–1356.

Gupta, D. K., Skali, H., Claggett, B., Kasabov, R., Cheng, S., Shah, A. M., Loehr, L. R., Heiss, G., Nambi, V., Aguilar, D., et al. (2014). Heart failure risk across the spectrum of ankle-brachial index: the aric study (atherosclerosis risk in communities). *JACC: Heart Failure*, 2(5):447–454.

impedimed (2022). https://www.impedimed.com/ sfb7.

Khalil, S. F., Mohktar, M. S., and Ibrahim, F. (2014). The theory and fundamentals of bioimpedance analysis in clinical status monitoring and diagnosis of diseases. *Sensors*, 14(6):10895–10928.

Kocbach, J., Folgerø, K., Mohn, L., and Brix, O. (2011). A simulation approach to optimizing performance of equipment for thermostimulation of muscle tissue using comsol multiphysics. *Biophysics and Bioengineering Letters*, 4(2):9–33.

MatWeb (2022). http://www.matweb.com/ AISI type 304 stainless steel.

Puertas, M., Giménez, L., Pérez, A., Scagliusi, S. F., Pérez, P., Olmo, A., Huertas, G., Medrano, J., and Yúfera, A. (2021). Modeling edema evolution with electrical bioimpedance: Application to heart failure patients. In *2021 XXXVI Conference on Design of Circuits and Integrated Systems (DCIS)*, pages 1–6. IEEE.

Różdżyńska-Świątkowska, A., Jurkiewicz, E., and Tylki-Szymańska, A. (2015). Bioimpedance analysis as a method to evaluate the proportion of fatty and muscle tissues in progressive myopathy in pompe disease. In *JIMD Reports, Volume 26*, pages 45–51. Springer.